Electronic Supplementary Material (ESI) for Environmental Science: Nano.

Supplementary information

Nonmonotonic relationship between the degradation of black phosphorus and its bioactivity in suppressing the centrosome polo-like kinase 1

Chaofan Deng,[a] Luyao Ren,[a] Lin Yang,[a] Xia Liu,[a] Yanhui Dai,[a] Jian Zhao,[ab] and Tongtao Yue*[ab]

[a] *Institute of Coastal Environmental Pollution Control, Key Laboratory of Marine Environment and Ecology, Ministry of Education, Ocean University of China, Qingdao 266100, China. E-mail: yuetongtao@ouc.edu.cn*

[b] *Laboratory of Marine Ecology and Environmental Science, Qingdao National Laboratory for Marine Science and Technology, Qingdao 266237, China*

Table S1. Forcefield parameters for black phosphorus.

Parameter	**Atom types**	**Value**
σ (Å)	P	3.33
ε (kcal mol^{-1})	P	0.4
k_r (kcal mol^{-1})	P	297
q (e)	O	-1.130
	P-O	1.626
	P-P-O	-0.406
	P-P-P-O	-0.106

The remaining P atoms located inside the black phosphorus are considered uncharged.

Table S2. The details of the simulation systems.

Simulation systems		Components	Simulation time (ns)
Control	**PBD**	PBD, H_2O (31494), Na^+ (62), Cl^- (61)	300
	PBD@Phosphopeptide	PBD, Phosphopeptide, H_2O (31450), Na^+ (65), Cl^- (61)	300
Initial stage of degradation	**PBD & P-BP**	PBD, P-BP, H_2O (105493), Na^+ (205), Cl^- (204)	300
	PBD & P-BP (back)	PBD, P-BP, H_2O (105812), Na^+ (205), Cl^- (204)	300
	PBD & BP-O	PBD, BP-O, H_2O (106240), Na^+ (290), Cl^- (204)	300
	PBD & BP-O (back)	PBD, BP-O, H_2O (106165), Na^+ (290), Cl^- (204)	300
	PBD & GN	PBD, GN, H_2O (106253), Na^+ (205), Cl^- (204)	300
	PBD & GO	PBD, GO, H_2O (105884), Na^+ (253), Cl^- (204)	300
Mid stage of degradation	**PBD & BP-QD(Site1)**	PBD, BP-QD, H_2O (31473), Na^+ (74), Cl^- (61)	100
	PBD & BP-QD(Site2)	PBD, BP-QD, H_2O (31447), Na^+ (74), Cl^- (61)	100
	PBD & BP-QD(Site3)	PBD, BP-QD, H_2O (31472), Na^+ (74), Cl^- (61)	100
	PBD & BP-QD*(Site1)	PBD, BP-QD*, H_2O (31469), Na^+ (62), Cl^- (61)	100
	PBD & BP-QD*(Site2)	PBD, BP-QD*, H_2O(31456), Na^+(62), Cl^- (61)	100
	PBD & BP-QD*(Site3)	PBD, BP-QD*, H_2O (31466), Na^+ (62), Cl^- (61)	100
	PBD@Phosphopeptide & BP-QD(Site1)	PBD, Phosphopeptide, BP-QD, H_2O (31386), Na^+ (77), Cl^- (61)	100
Final stage of degradation	**PBD & PO_3^{3-}**	PBD, PO_3^{3-} (30), H_2O (31308), Na^+ (152), Cl^- (61)	100
	PBD & PO_4^{3-}	PBD, PO_4^{3-} (30), H_2O (31297), Na^+ (152), Cl^- (61)	100
	PBD@Phosphopeptide & PO_3^{3-}	PBD, Phosphopeptide, PO_3^{3-} (30), H_2O (31263), Na^+ (155), Cl^- (61)	100
	PBD@Phosphopeptide & PO_4^{3-}	PBD, Phosphopeptide, PO_4^{3-} (30), H_2O (31265), Na^+ (155), Cl^- (61)	100

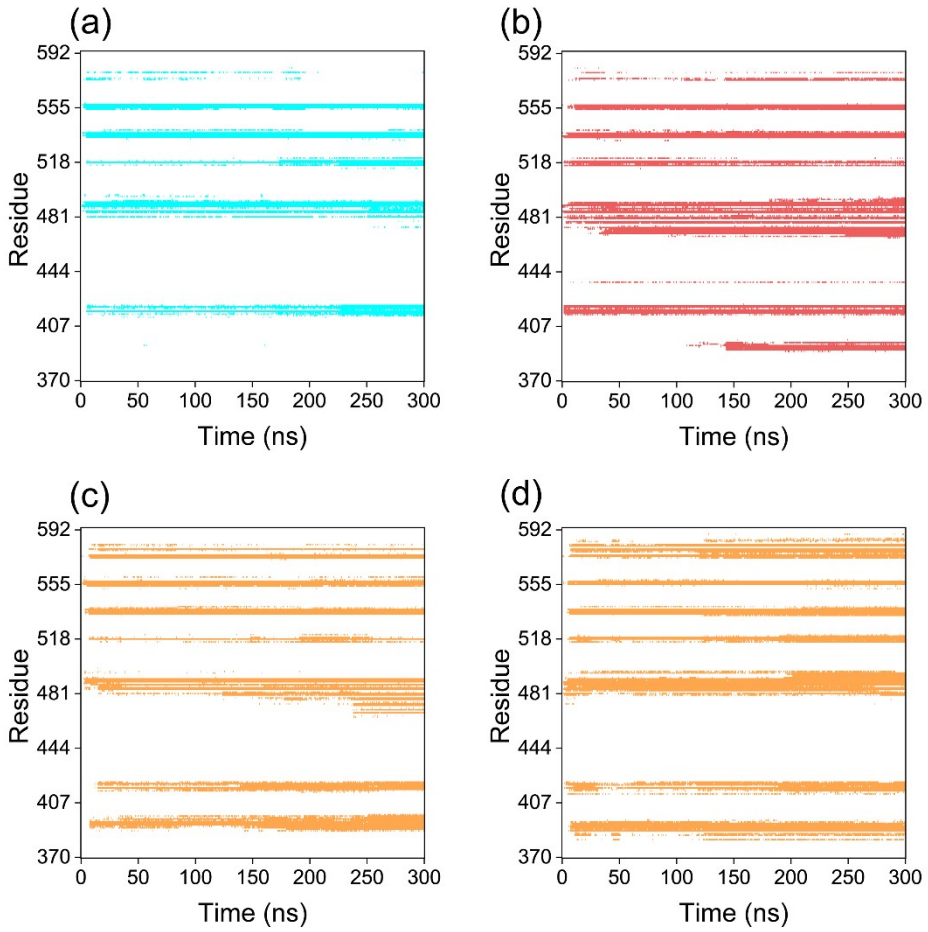

Figure S1. Time evolutions of the amino acid residues in contact with nanosheets of P-BP (a), BP-O (b), GN (c), and GO (d).

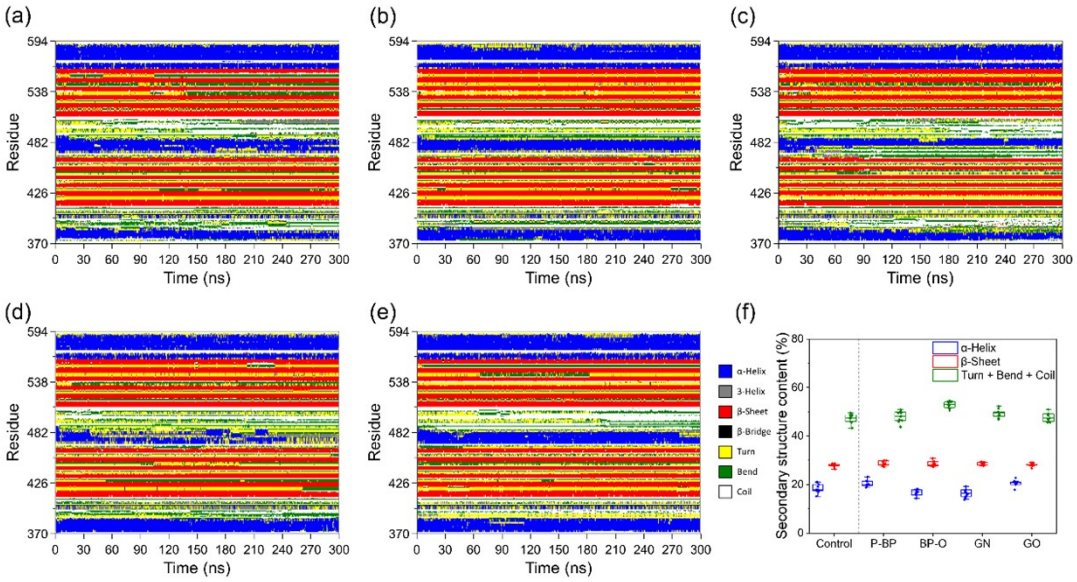

Figure S2. The secondary structure change diagram of different systems: (a) Control, (b) P-BP, (c) BP-O, (d) GN, and (e) GO. (f) Secondary structure content of each system.

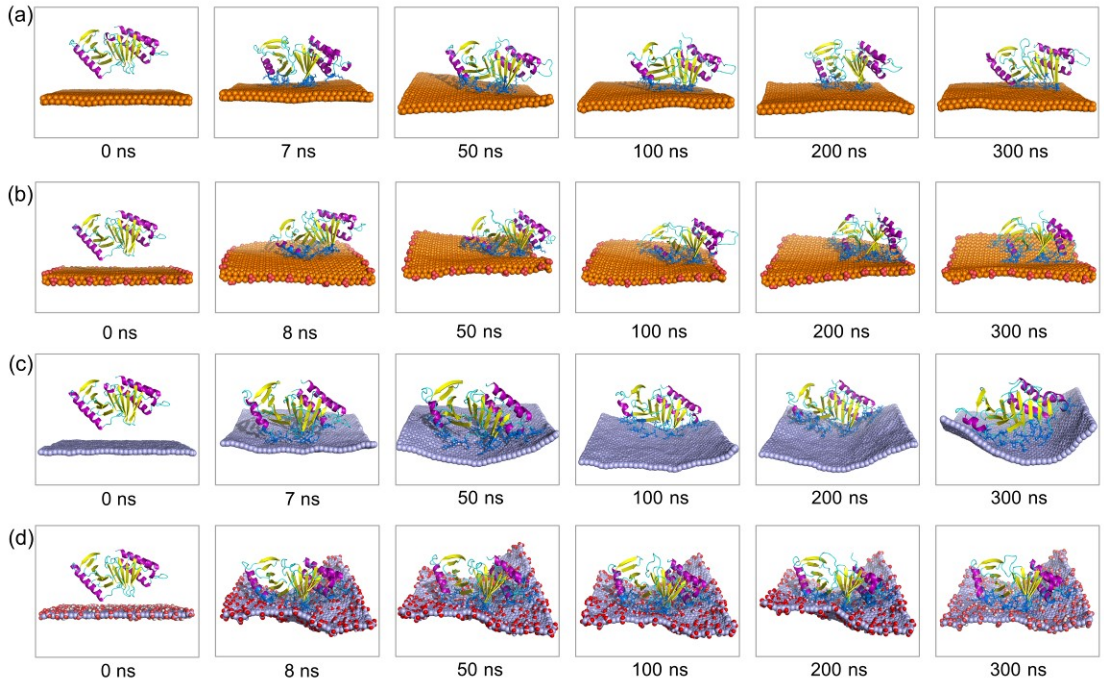

Figure S3. Time sequences of typical snapshots depicting interactions of PBD with nanosheets of P-BP (a), BP-O (b), GN (c), and GO (d). Amino acid residues bound to nanomaterials are displayed in blue stick models.

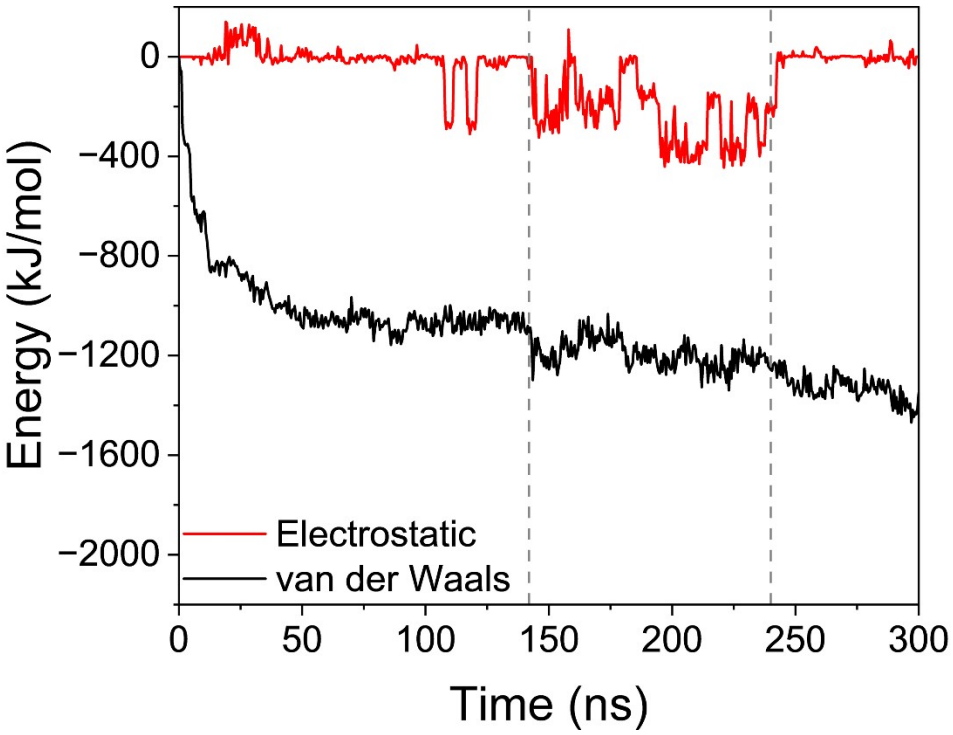

Figure S4. Time evolutions of the van der Waals and electrostatic interaction energies between PBD and BP-O.

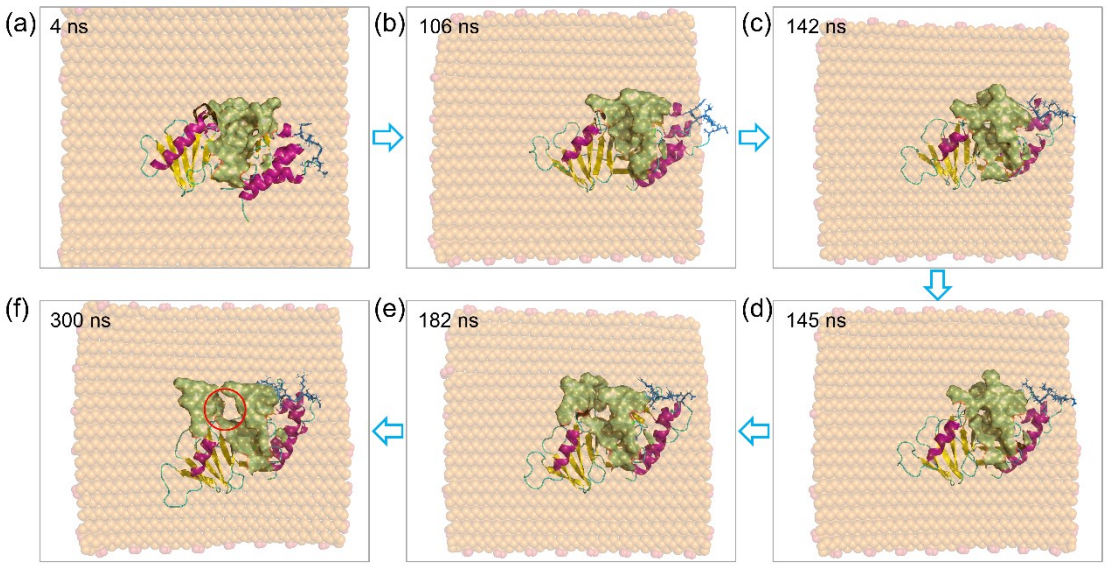

Figure S5. Bottom views of the snapshots at different times illustrating distortion of the PBD's active pocket induced by interactions with BP-O.

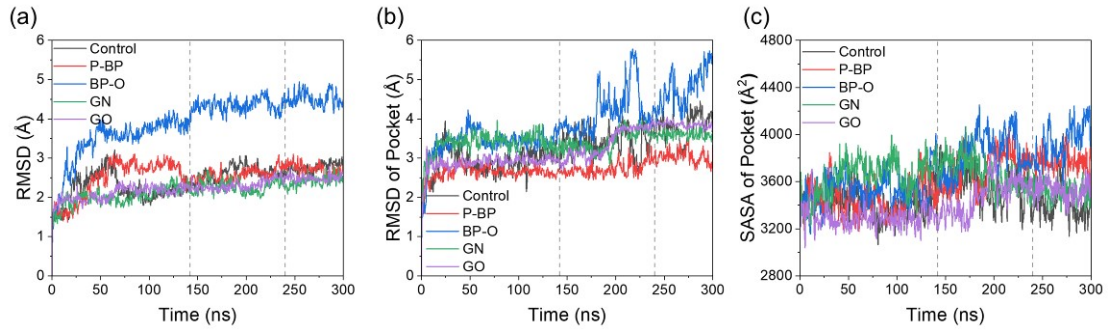

Figure S6. Comparison of the protein's conformation change induced by interactions with different nanomaterials. (a, b) Time evolutions of the root mean square deviation (RMSD) for the entire protein (a) and the PBD's pocket (b). (c) Time evolutions of the solvent accessible surface area (SASA) for the PBD's pocket.

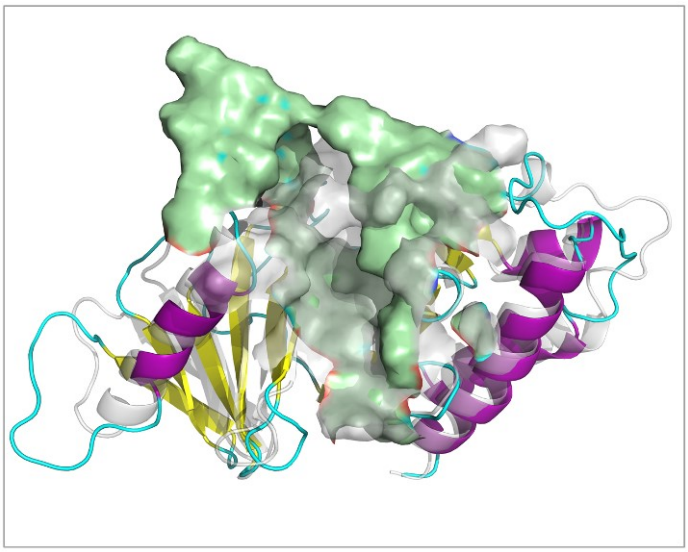

Figure S7. Distortion of the PBD's active pocket induced by interactions with BP-O. The reference configuration not affected by BP-O is displayed in white and transparent, while the pocket region after interactions with BP-O is displayed in green.

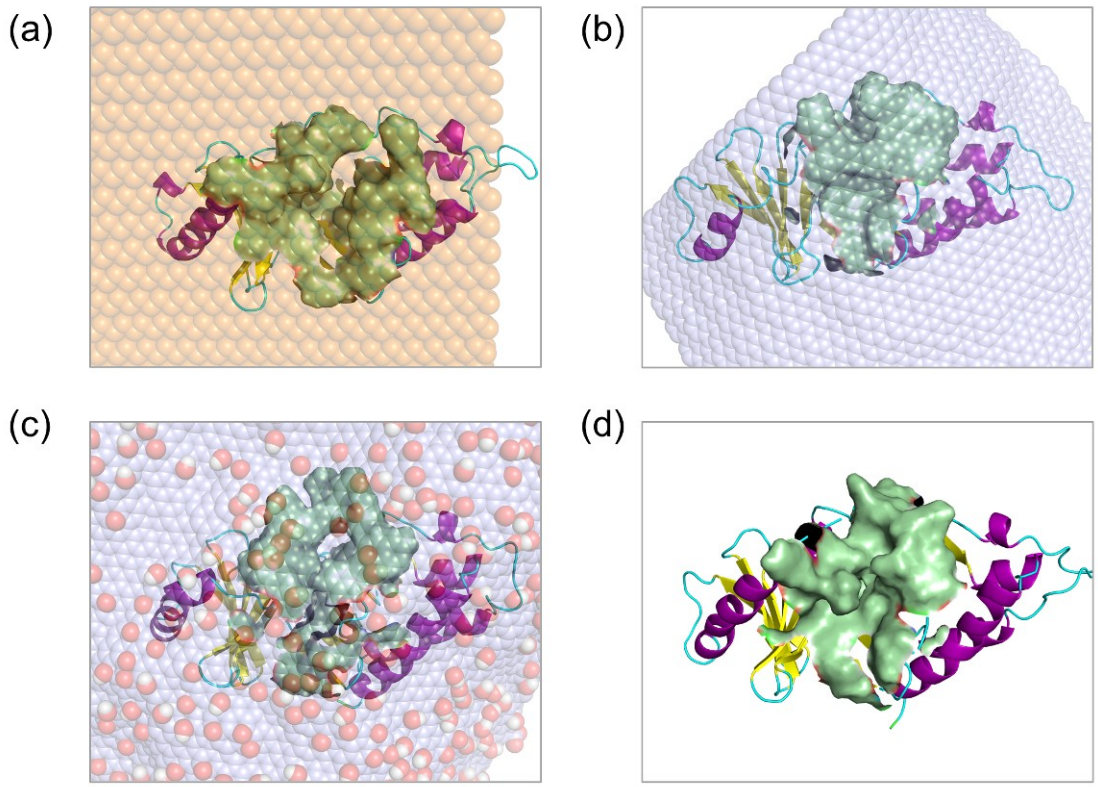

Figure S8. The PBD's pocket remained intact after interactions with P-BP (a), GN (b), and GO (c). The pure protein in equilibrium is shown for comparison (d). Residues in the PBD's pocket are colored in mustard.

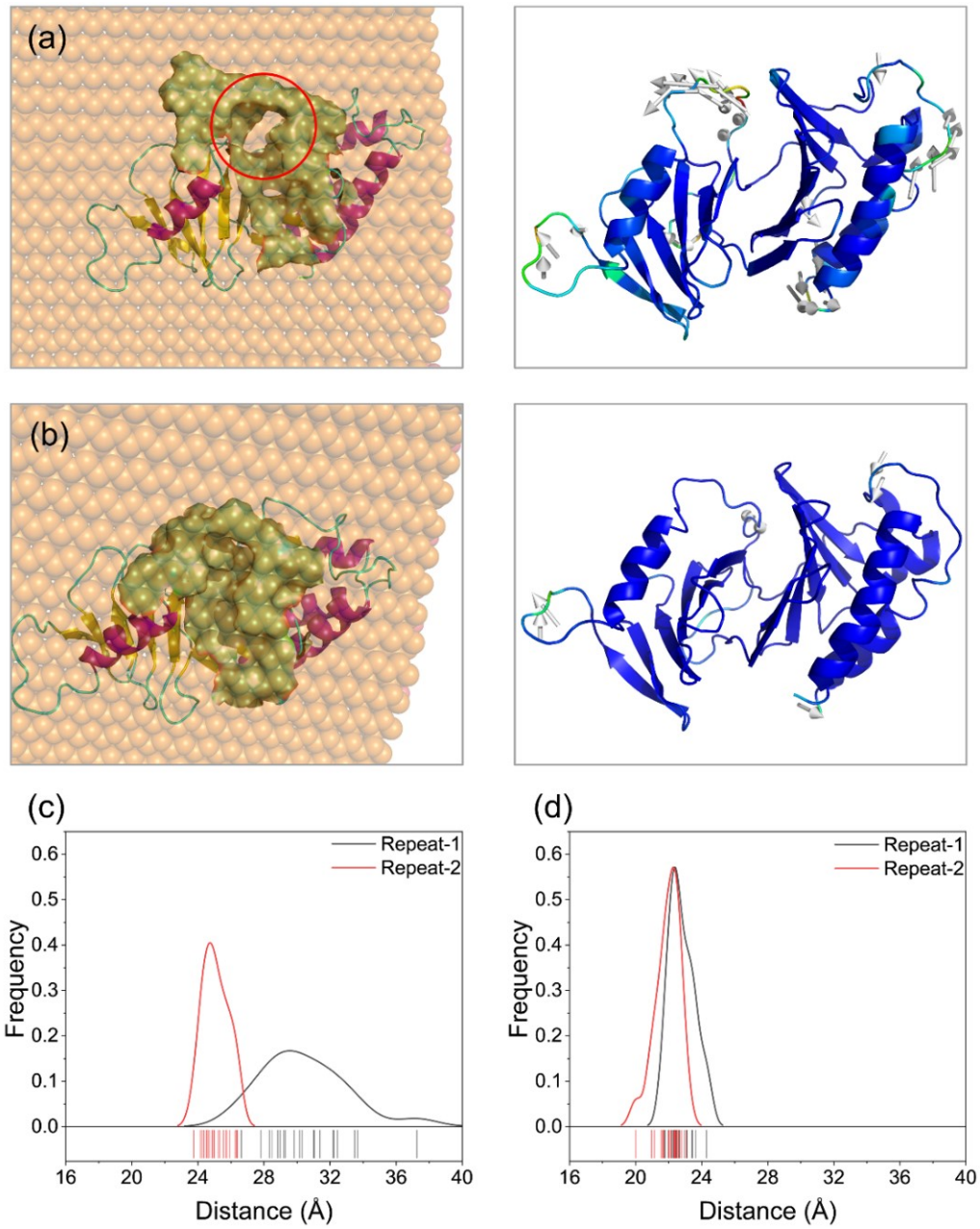

Figure S9. Repeated simulations reproducing the distortion of the PBD's pocket induced by interactions with BP-O via a lever-like mechanism. (a, b) Bottom views of the PBD interactions with PB-O. The right panel is the RMSF-Vector diagram colored by the values of b-factor, showing flexibility and movement of residues. White arrows indicate the direction of residues' relative movement. The distortion of the PBD's pocket in one repeated simulation is marked with a red circle (a). (c, d) Frequency distributions of two distances between diagonal residues in the PBD's pocket characterizing degree of the pocket distortion.

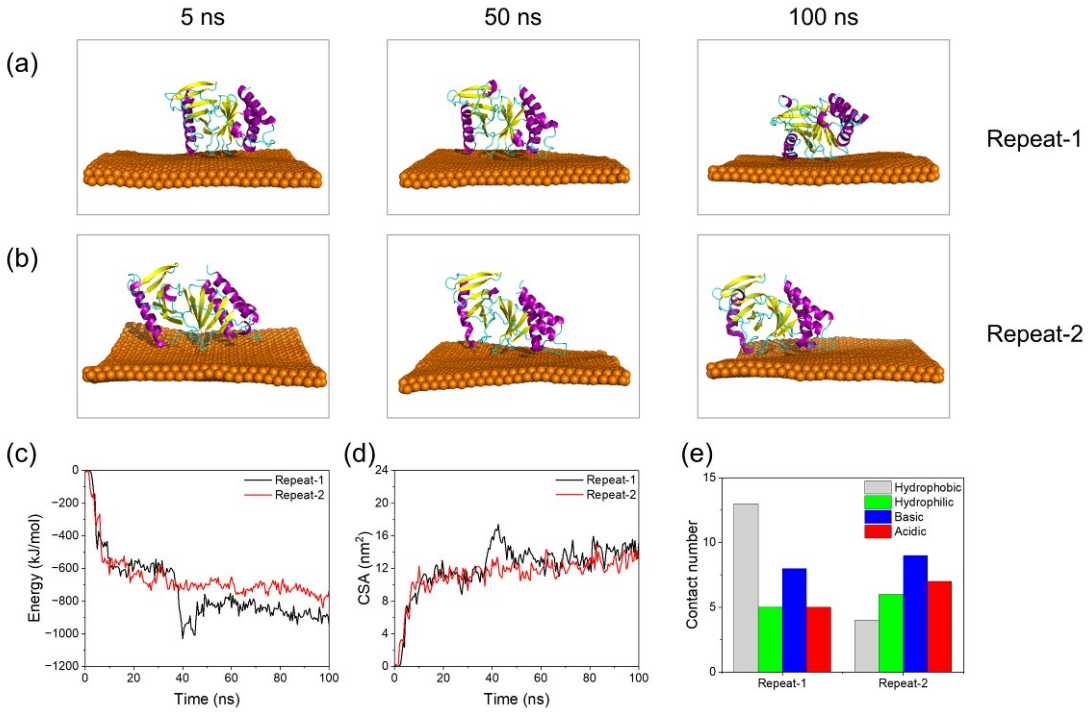

Figure S10. Repeated simulations of PBD interactions with P-BP. (a, b) Time sequences of typical snapshots depicting interactions of PBD with P-BP. (c) Time evolutions of the interaction energies between PBD and P-BP. (d) Time evolutions of the contact surface area (CSA) between PBD and P-BP. (e) Numbers of different residues in contact with P-BP.

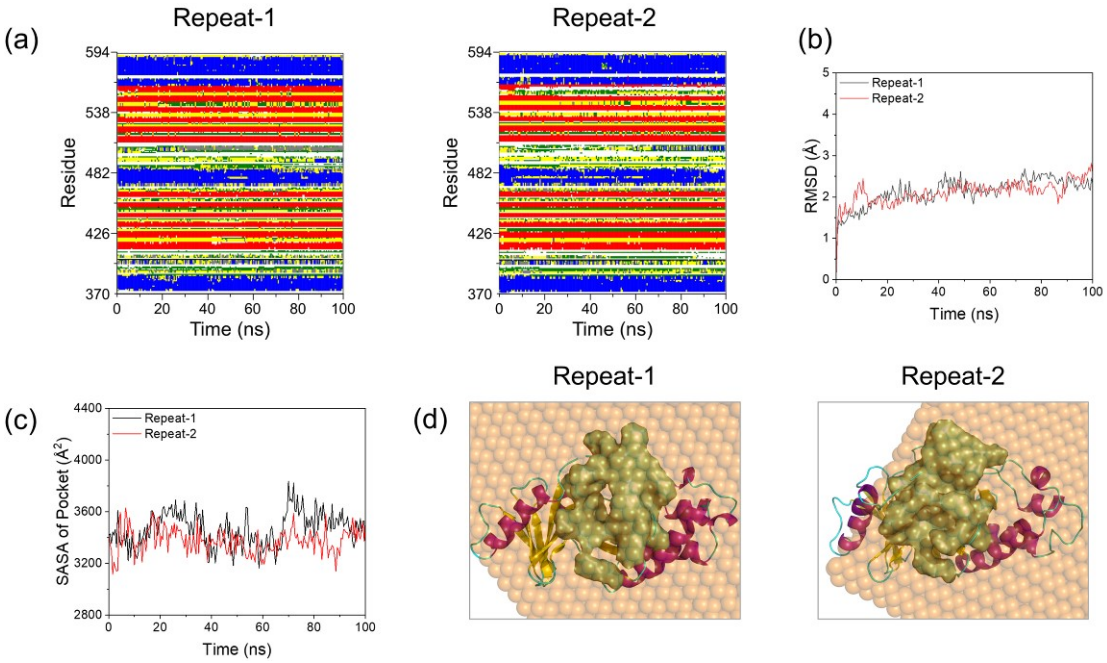

Figure S11. Repeated simulations to confirm the insignificant effect of P-BP on the structure of the PBD. (a) The secondary structure change diagram of PBD interacting with P-BP in two simulations. (b) Time evolutions of the RMSD for PBD interacting with P-BP. (c) Time evolutions of the solvent accessible surface area (SASA) for the PBD's pocket. (d) Snapshots of the pocket structure of PBD after interactions with P-BP.

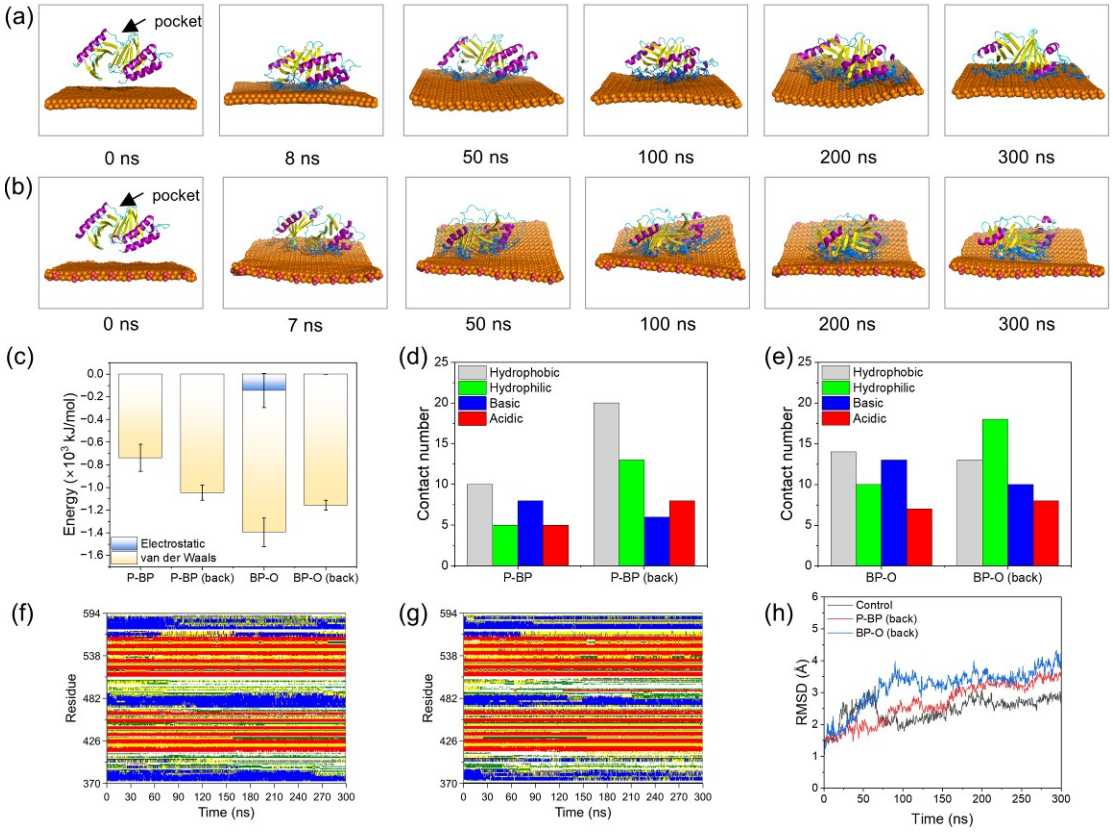

Figure S12. Effect of the initial contact mode on PBD interactions with P-BP and BP-O. (a, b) Time sequences of typical snapshots depicting PBD interactions with P-BP (a) and BP-O (b) with the nanosheets positioned behind the PBD's pocket. Residues in contacts with nanosheets are displayed in blue stick models. (c) The interaction energy between nanomaterials and PBD with different initial contact modes. (d, e) Numbers of different residues in contact with P-BP (d) and BP-O (e) with different orientations. (f, g) The secondary structure change diagram of PBD interacting with P-BP (f) and BP-O (g). (h) Time evolutions of the RMSD for PBD interacting with two nanosheets with opposite orientations.

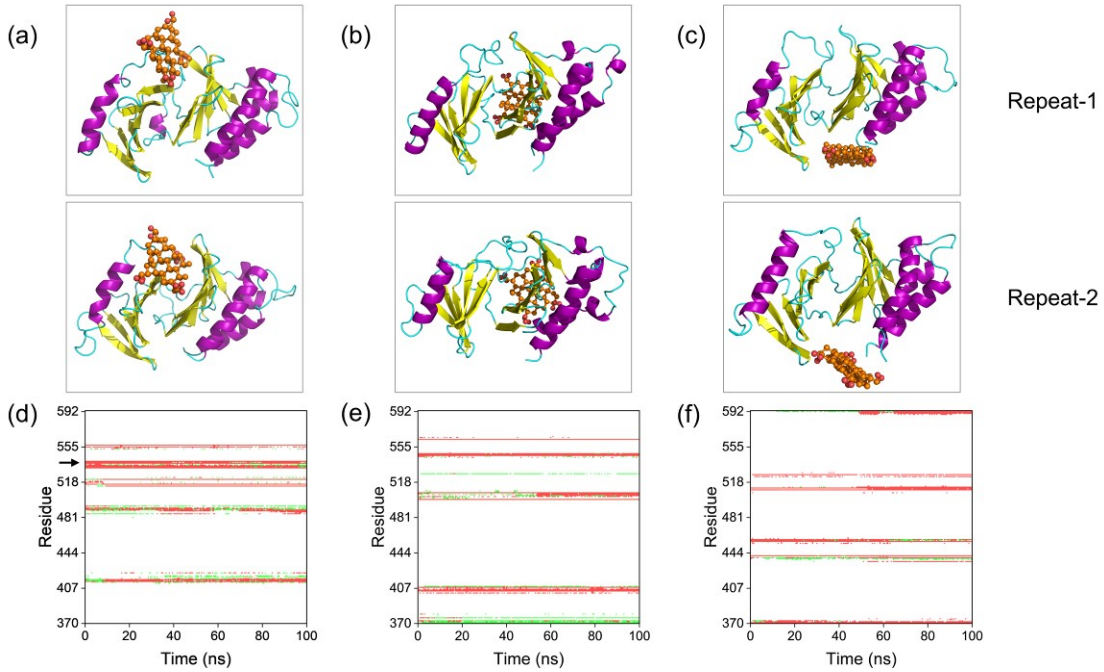

Figure S13. Repeated simulations of stable binding of BP-QD to PBD. (a-c) Typical snapshots of the binding of BP-QD to the PBD at Site1 (a), Site2 (b), and Site3 (c) in two parallel simulations. (d-f) Time evolutions of residues in contact with BP-QD at Site1 (d), Site2 (e), and Site3 (f). Repeat-1 is shown in red, while Repeat-2 is shown in green.

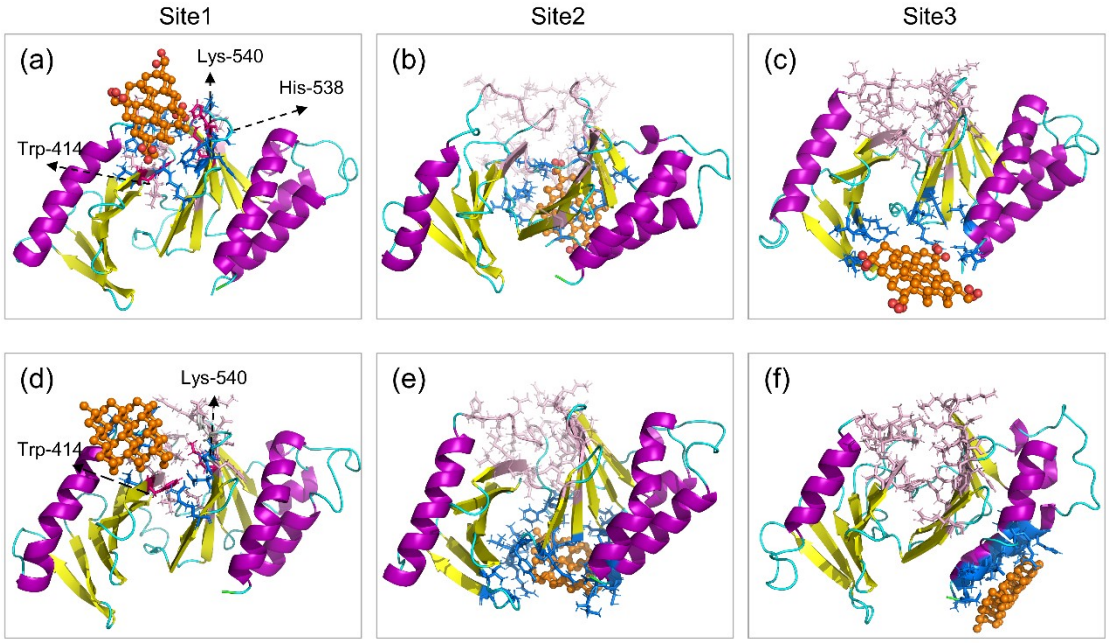

Figure S14. Binding conformations of BP-QD and BP-QD* with PBD at three different sites obtained through 100 ns MD simulations. (a-c) BP-QD at three sites of PBD, (d-f) BP-QD* at the same three sites. Residues constituting active pocket are displayed in the bright pink stick model, and residues bound to quantum dots are highlighted in the blue stick model. The three important residues (Trp-414, His-538, Lys-540) in the pocket are highlighted with magenta color.

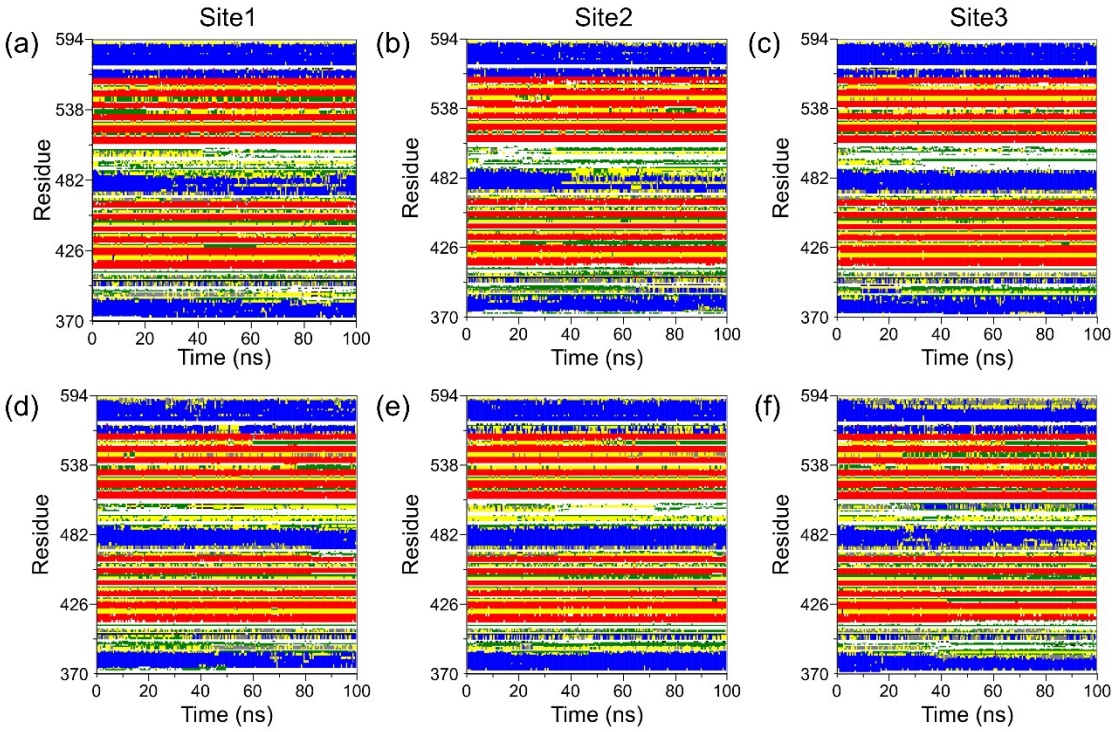

Figure S15. The secondary structure change diagram of PBD during interactions with BP-QD (a-c) and BP-QD* (d-f) in three different sites.

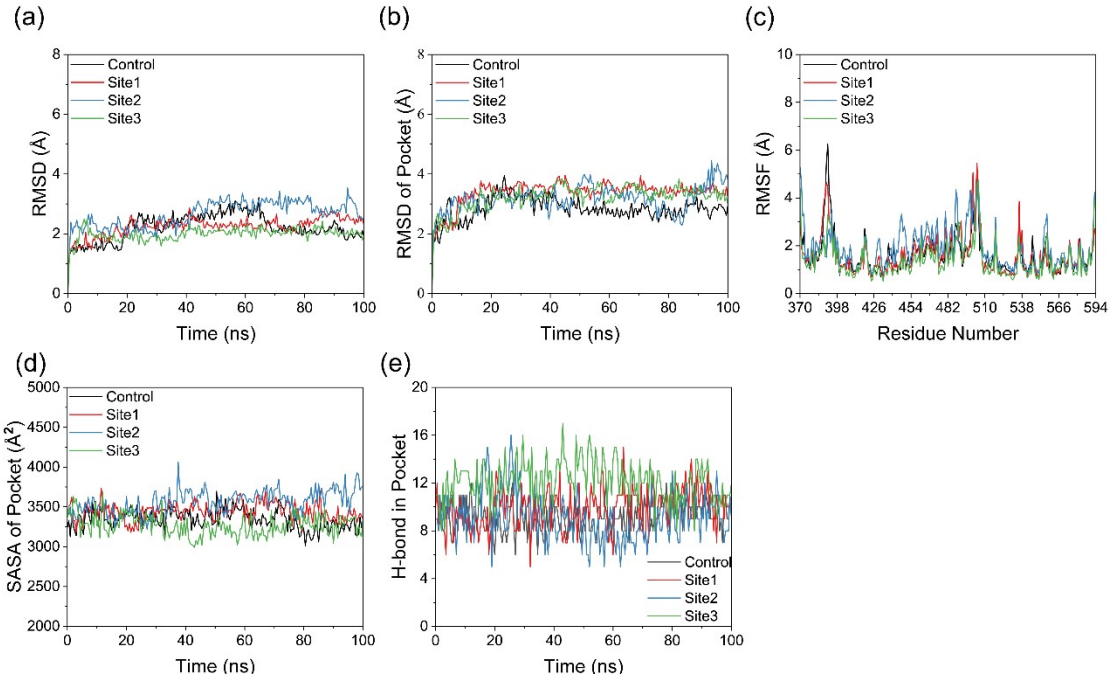

Figure S16. Comparison of the PBD's conformational change induced by interactions with BP-QD in three different sites. (a) RMSD of the entire protein. (b) RMSD of the PBD's pocket. (c) RMSF of residues after interactions with BP-QD. (d) SASA of the PBD's pocket during interactions with BP-QD. (e) The number of hydrogen bonds formed between residues in the PBD's pocket during interactions with BP-QD.

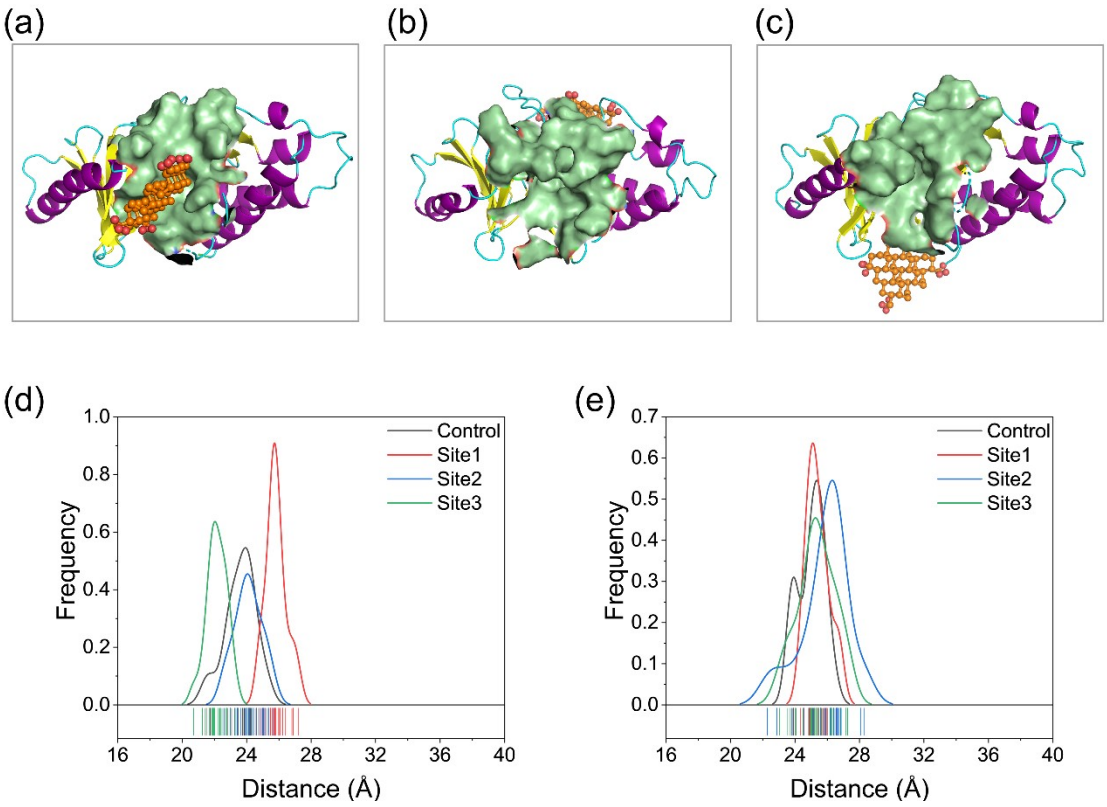

Figure S17. BP-QD induced no apparent change in the PBD's pocket structure. (a-c) Equilibrium structures of BP-QD docking to three sites of PBD with residues in the pocket colored in mustard. (d, e) Two distances between diagonal residues in the active pocket after interactions with BP-QD.

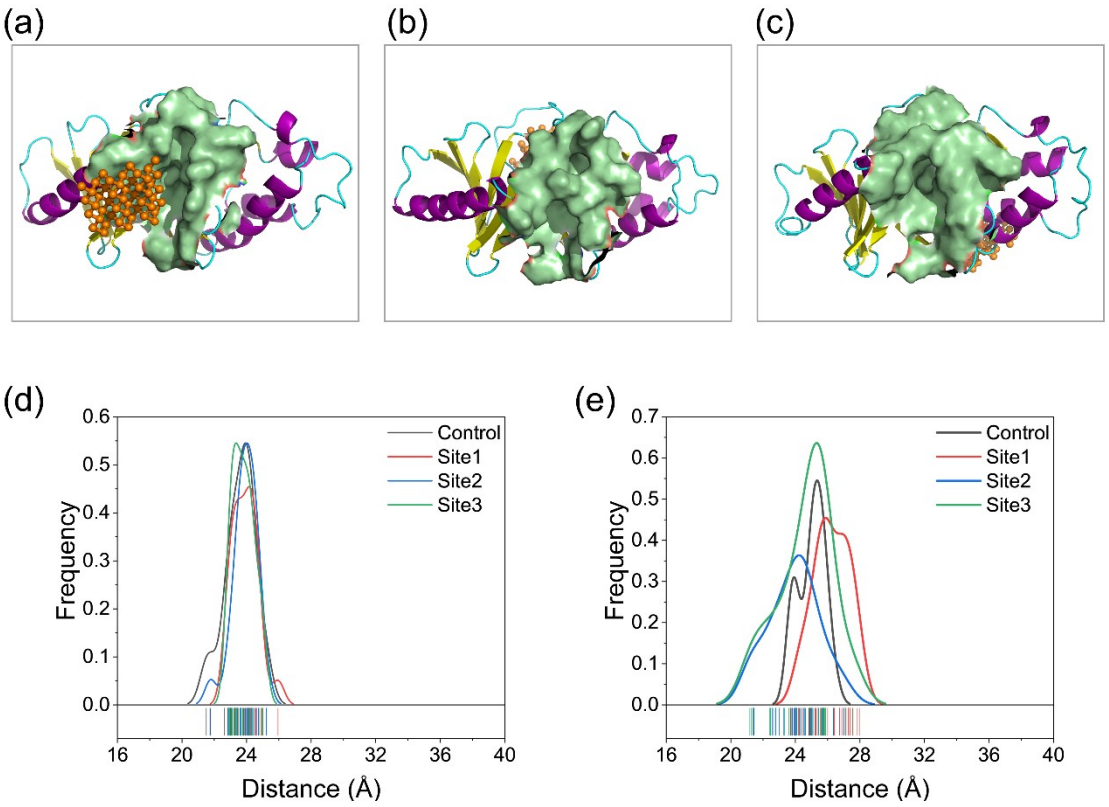

Figure S18. BP-QD* induced no apparent change in the PBD's pocket structure. (a-c) Equilibrium structures of BP-QD* docking to three sites of PBD with residues in the pocket colored in mustard. (d, e) Two distances between diagonal residues in the active pocket after interactions with BP-QD*.

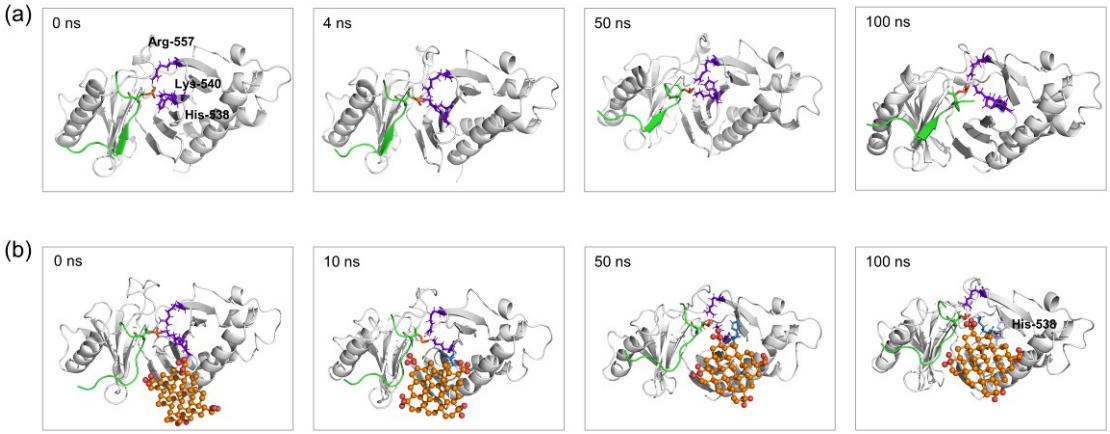

Figure S19. Effect of BP-QD on the binding of phosphopeptide to the PBD's pocket. (a) Typical snapshots of a phosphopeptide (green) binding to the PBD's pocket. (b) With addition of BP-QD, His-538 lost its stable binding to the phosphopeptide. Vital amino acid residues that only bind to phosphopeptide are displayed in purple. Residues that bind to both phosphopeptide and BP-QD are displayed in blue. Residues that captured by BP-QD are displayed in light blue. Phosphate group in phosphopeptide is shown as stick model.

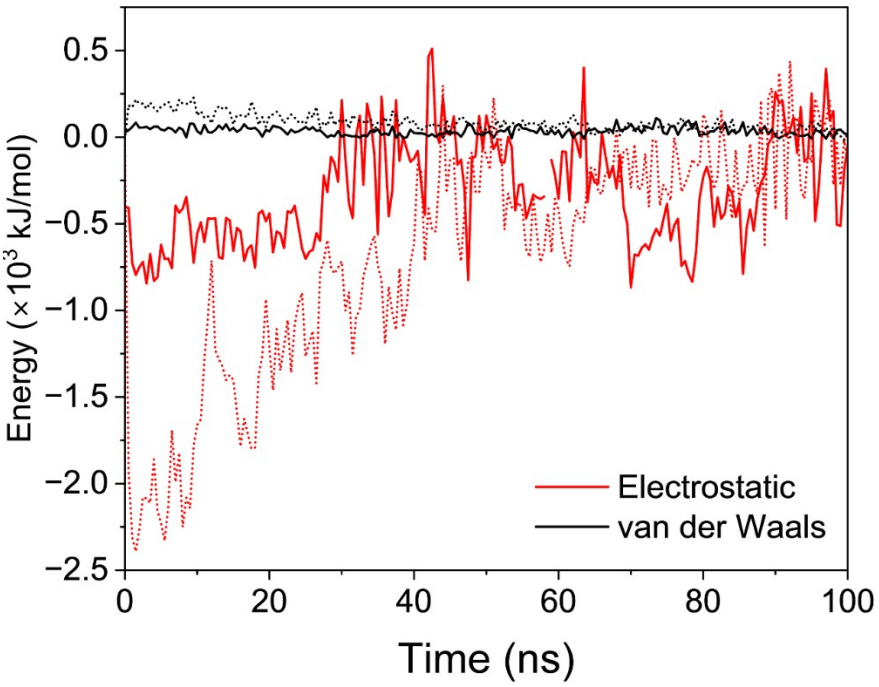

Figure S20. Time evolutions of the van der Waals and electrostatic interaction energies between PBD and two types of phosphate ions. The solid lines represent PO_3^{3-}, while the dotted lines represent PO_4^{3-}.

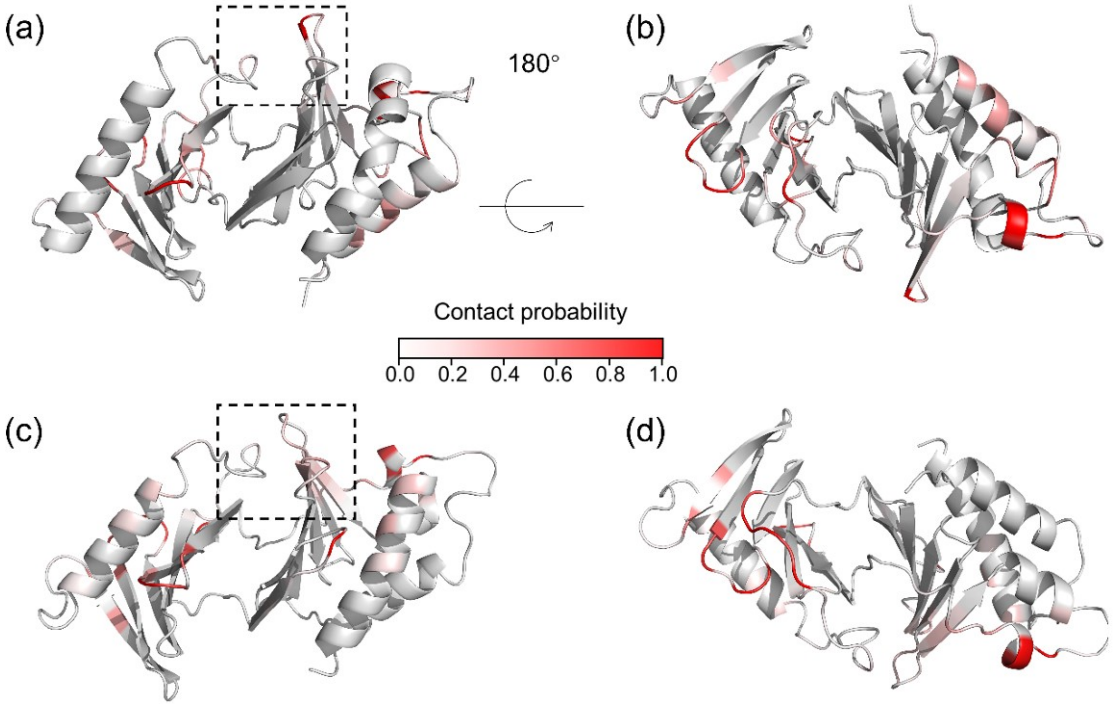

Figure S21. Map of the contact probability between PO_x^{3-} and PBD. (a, b) PO_3^{3-} , (c-d) PO_4^{3-} . The active pocket of PBD is labeled by the black dashed line.

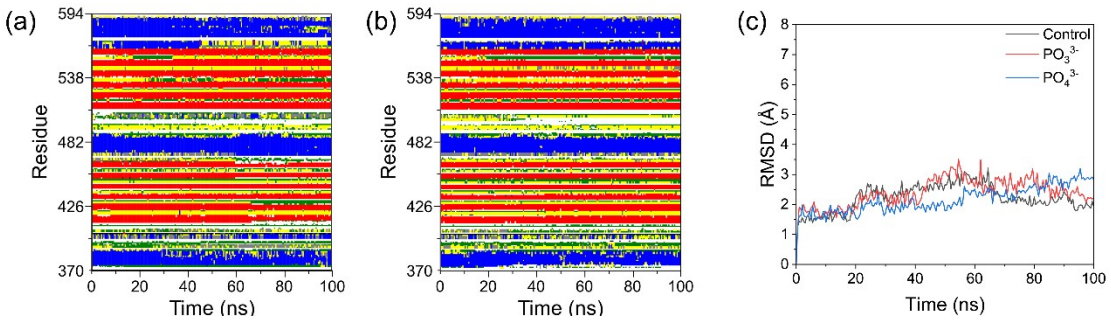

Figure S22. No apparent change in the PBD's structure was induced by interactions with phosphate ions. (a, b) The secondary structure of PBD during interactions with PO_3^{3-} (a) and PO_4^{3-} (b). (c) Time evolutions of the PBD's RMSD during interactions with phosphate ions.

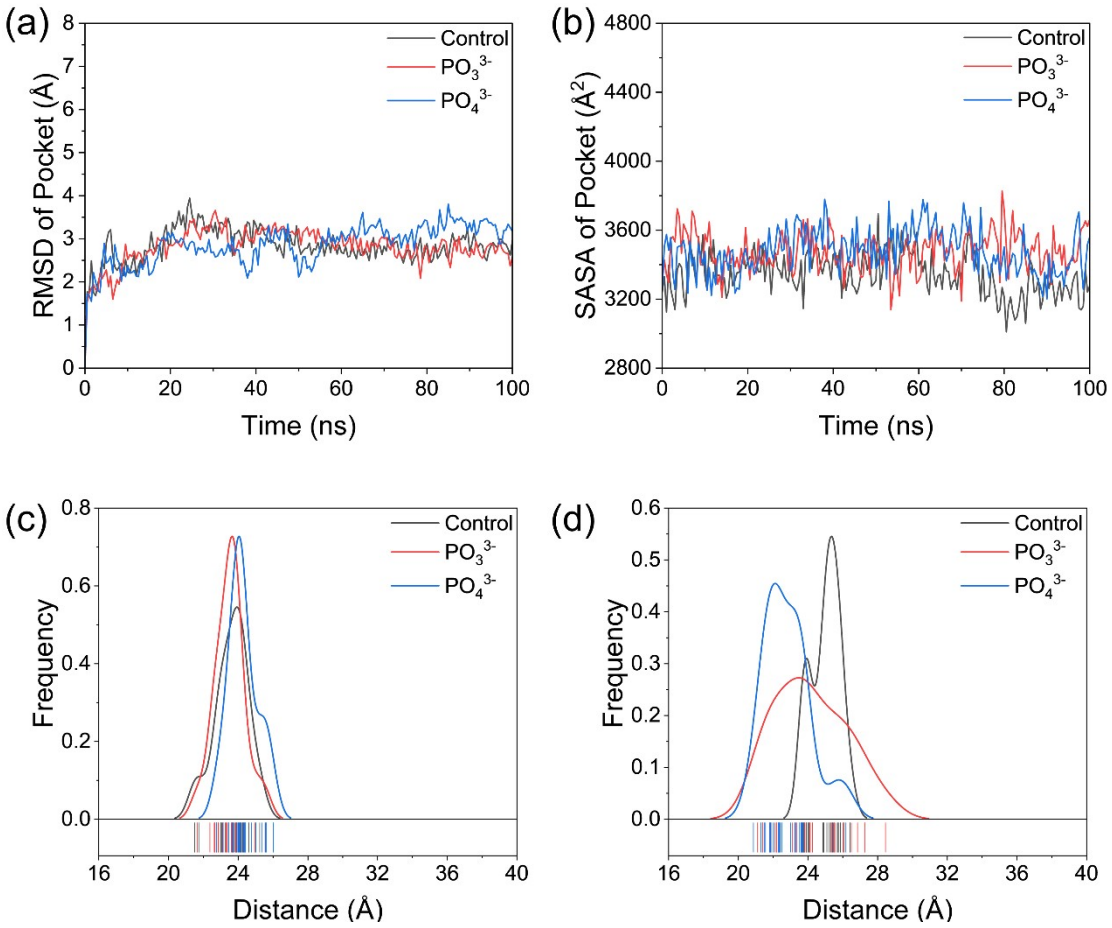

Figure S23. (a, b) Time evolutions RMSD (a) and SASA (b) of the PBD's active pocket during interactions with phosphate ions. (c, d) The distances between diagonal residues in the active pocket after interactions with phosphate ions.

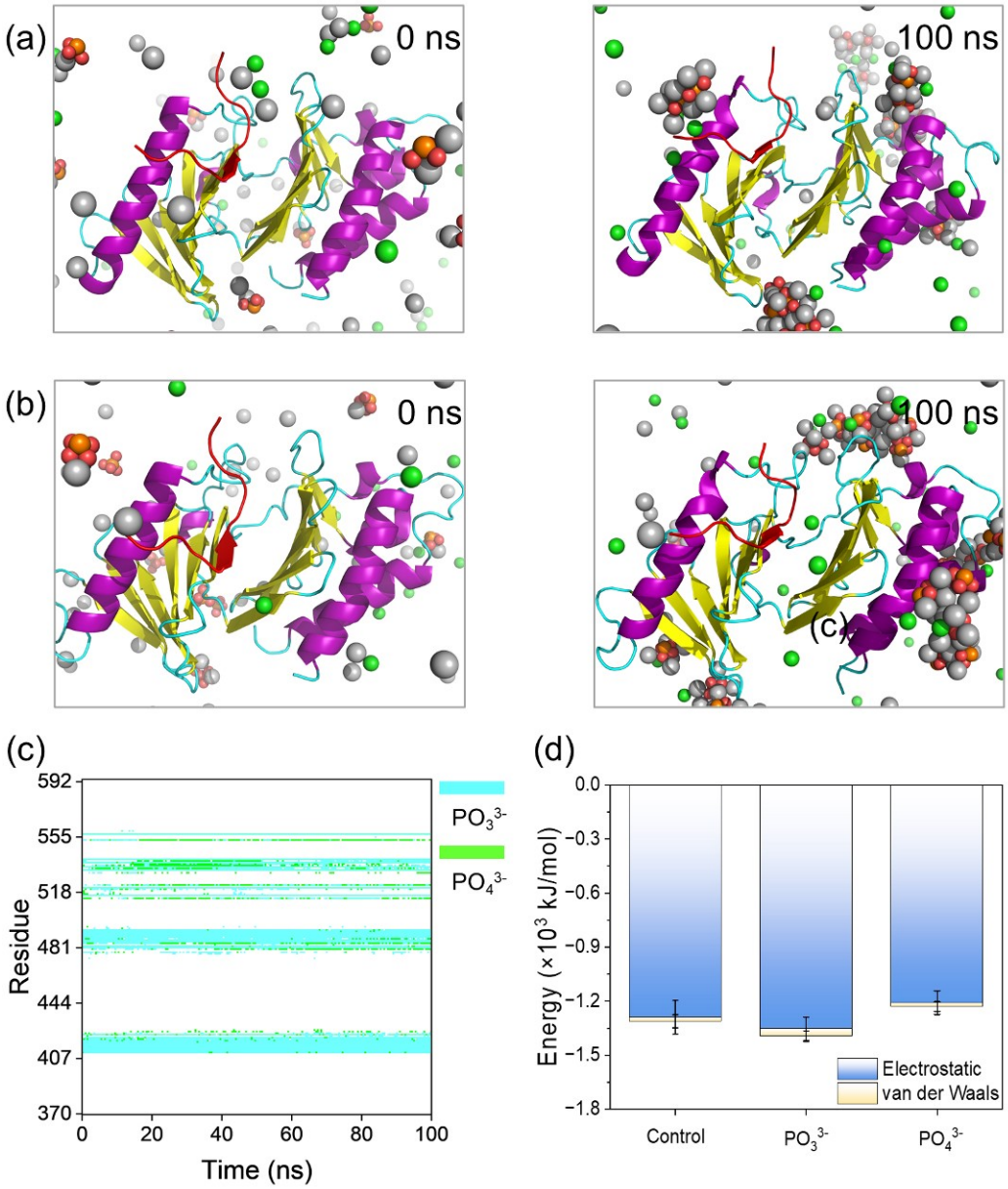

Figure S24. Minor effect of phosphate ions on the binding of phosphopeptide to the PBD's pocket. (a, b) Initial and final state of interactions with PO_3^{3-} (a) and PO_4^{3-} (b) ions. (c) Time evolutions of residues in contact with phosphopeptide in the presence of phosphate ions. (d) Interaction energies between PBD and phosphopeptide with and without phosphate ions.